2010

Design Sensitivities of the Superconducting Parallel-Bar Cavity

Subashini U. De Silva
Old Dominion University, pdesilva@odu.edu

Jean Delayen
Old Dominion University, jdelayen@odu.edu

Original Publication Citation

De Silva, S. U., & Delayen, J. (2010). Design sensitivites of the superconducting parallel-bar cavity. *In Proceedings of Linear Accelerator Conference LINAC2010* (812-814). Joint Accelerator Conferences Website. https://accelconf.web.cern.ch/LINAC2010/papers/thp024.pdf

DESIGN SENSITIVITIES OF THE SUPERCONDUCTING PARALLEL-BAR CAVITY*

S.U. De Silva[1,2#], J.R. Delayen[1,2],
[1]Center for Accelerator Science, Old Dominion University, Norfolk, VA 23529, U.S.A.
[2]Thomas Jefferson National Accelerator Facility, Newport News, VA 23606, U.S.A.

Abstract

The superconducting parallel-bar cavity has properties that makes it attractive as a deflecting or crabbing rf structure. For example it is under consideration as an rf separator for the Jefferson Lab 12 GeV upgrade and as a crabbing structure for a possible LHC luminosity upgrade. In order to maintain the purity of the deflecting mode and avoid mixing with the near accelerating mode caused by geometrical imperfection, a minimum frequency separation is needed which depends on the expected deviations from perfect symmetry. We have done an extensive analysis of the impact of several geometrical imperfections on the properties of the parallel-bar cavities and the effects on the beam, and present the results in this paper.

INTRODUCTION

The superconducting parallel-bar cavity [1] has been optimized to meet the requirements of net deflection and dimensional constraints for the applications of 499 MHz deflecting cavity for Jefferson Lab 12 GeV upgrade and the crabbing cavity for the LHC luminosity upgrade operating at 400 MHz. The optimized 499 MHz and 400 MHz designs are shown in Fig. 1. A detailed optimization [2] carried out on the parallel-bar cavity shows that the compact design has lower surface fields, and high shunt impedance compared to other deflecting and crabbing structures. Further analysis of HOM properties [3] performed on the design shows the existence of only higher order modes where the fundamental deflecting mode has the lowest frequency. The cavity properties of the two designs are shown in Table 1.

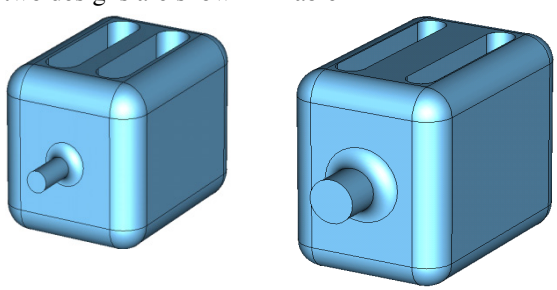

Figure 1: Optimized 499 MHz (left) 400 MHz (right) parallel-bar structures.

Table 1: Properties of Parallel-bar Structures

Parameter	499 MHz	400 MHz	KEK Cavity[4]	Units
Freq. of π mode	499.2	400.0	501.7	MHz
λ/2 of π mode	300.4	374.7	299.8	mm
Freq. of 0 mode	517.8	411.0	~ 700.0	MHz
Cavity length	394.4	444.7	299.8	mm
Cavity width	290.0	300.0	866.0	mm
Cavity height	304.8	383.2	483.0	mm
Bars width	67.0	55.0	-	mm
Bars length	284.0	330.0	-	mm
Aperture diameter	40.0	84.0	130.0	mm
Deflecting voltage (V_T^*)	0.3	0.375	0.3	MV
Peak electric field (E_P^*)	1.85	2.2	4.32	MV/m
Peak magnetic field (B_P^*)	6.69	7.9	12.45	mT
Energy content (U^*)	0.031	0.271	-	J
Geometrical factor	67.96	74.1	220	Ω
$[R/Q]_T$	933.98	413.34	46.7	Ω
$R_T R_S$	6.3×10^4	2.06×10^4	1.03×10^4	Ω^2

At E_T^* = 1 MV/m

Mechanical deformations in any cavity design may lead to variations in the electro-magnetic field and properties of the cavity. Furthermore imperfections leading to asymmetries on the cavity structure may also affect the final achievable gradient from the cavity. The large flat surfaces of the geometry make the parallel-bar structure prone to deformations. These deformations may occur during fabrication and while in operation. Hence a comprehensive analysis of different cavity imperfections on the parallel-bar cavity is performed.

ANALYSIS OF DESIGN ASYMMETRIES

The parallel-bar cavity has two fundamental degenerate modes identified as the deflecting mode (π mode) and the accelerating mode (0 mode). The degeneracy in frequency is eliminated with the inclusion of the beam aperture and curving the edges of the cavity. The main contribution to the resultant deflection in the deflecting mode is by the transverse electric field between the bars, with zero longitudinal electric field. However various asymmetries in the design introduce a longitudinal electric field in the deflecting mode, leading to a mixing of the two modes.

Simulation Results

The amount of longitudinal electric field present due to different geometrical asymmetries as shown in Fig. 2 is analyzed for the 499 MHz parallel-bar cavity using CST Microwave Studio.

*Authored by Jefferson Science Associates, LLC under U.S. DOE Contract No. DE-AC05-06OR23177. The U.S. Government retains a non-exclusive, paid-up, irrevocable, world-wide license to publish or reproduce this manuscript for U.S. Government purposes.
Part of this work was done in collaboration with and supported by Niowave Inc. under the DOE STTR Phase I program.
#sdesilva@jlab.org

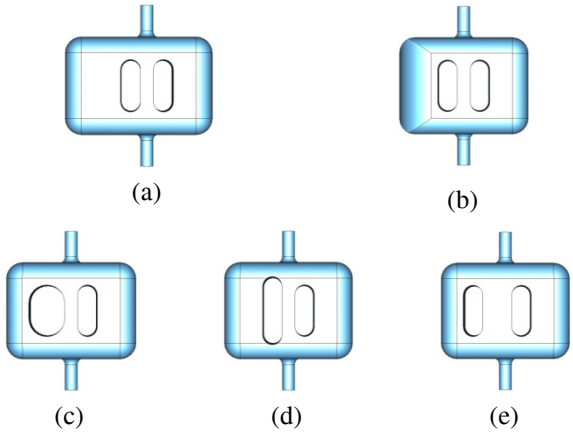

Figure 2: Parallel-bar designs with geometrical asymmetries by (a) cavity width (b) curving radius of edges (c) bar width (d) bar length and (e) separation between parallel bars.

The frequency separation between the two fundamental modes is mainly due to the curving radius of the cavity edges. Therefore the dependence of the curving radius of the cavity edges on mixing at different asymmetries is analyzed as shown in Fig. 3. The mixing for each asymmetry is evaluated for deviations of ± 5 mm. The amount of mixing is quantified by the ratio of V_Z/V_T given by

$$\frac{V_Z}{V_T} = \frac{\int_{-\infty}^{+\infty} j\vec{E}_Z(z, x=0)\, e^{-\frac{j\omega z}{c}}\, dz}{\int_{-\infty}^{+\infty} \left[\vec{E}_T(z, x=0) + j\left(\vec{v}\times\vec{B}(z, x=0)\right)_T\right] e^{-\frac{j\omega z}{c}}\, dz} \quad (1)$$

The curving radius of the edges of the parallel-bar cavity has no relative dependence on the mixing of the modes due to geometrical asymmetries. The imperfection in the separation between the parallel bars has the highest contribution to mixing of modes of 3% which is low.

The consequent effect on the frequency separation, in the two fundamental modes of the parallel-bar cavity due to the asymmetry in parallel-bar separation is shown in Fig. 4. The maximum change in frequency separation due to mixing is less than 1 MHz thus the effect on the required separation is minimal.

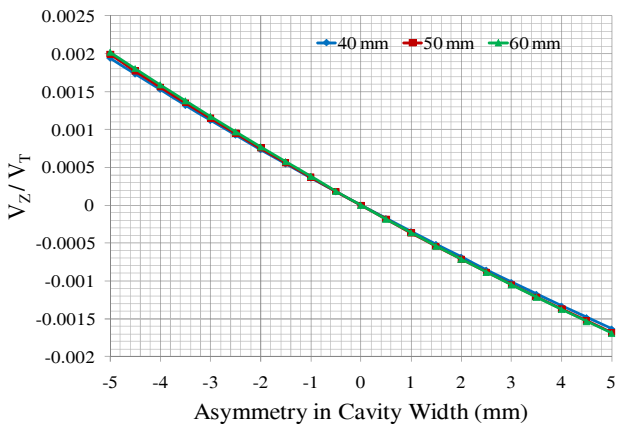

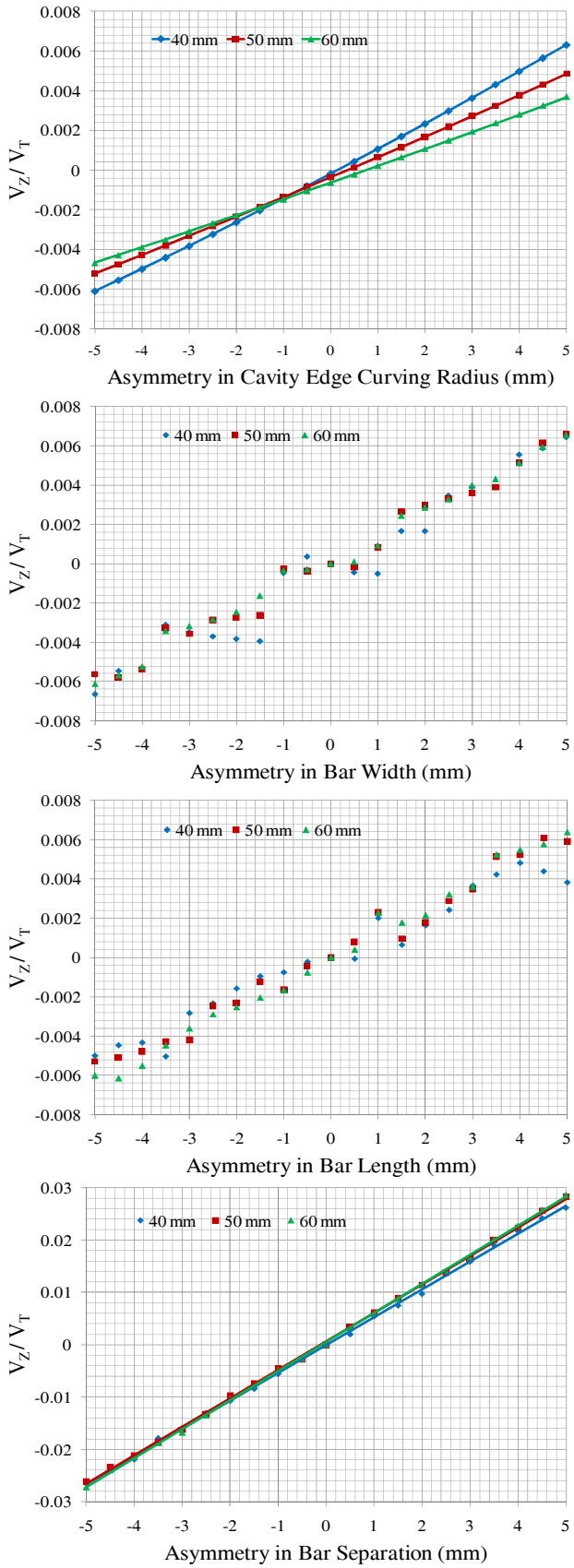

Figure 3: V_Z/V_T for different geometrical asymmetries with varying curving radius of cavity edges.

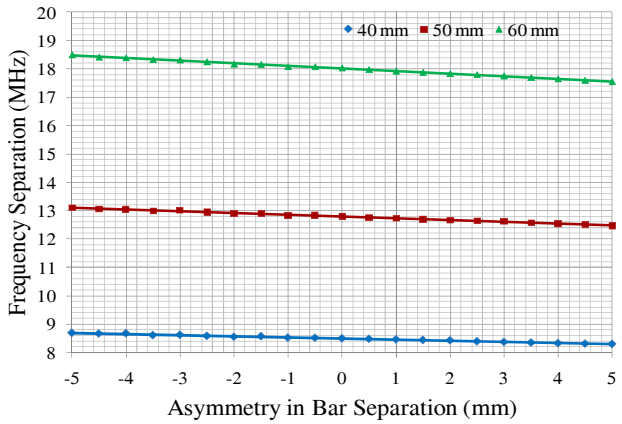

Figure 4: Frequency separation for the asymmetry in separation of parallel bars with varying curving radius of cavity edges.

Field Analysis

The maximum transverse (V_T) and longitudinal (V_Z) voltages in the parallel-bar cavity are given by Eq. 2 and 3 respectively.

$$V_T^{\max} = \left| \int_{-\infty}^{+\infty} \left[E_x(z)\cos(\omega t + \phi) + cB_y(z)\sin(\omega t + \phi) \right] dz \right| \quad (2)$$

$$V_Z^{\max} = \left| \int_{-\infty}^{+\infty} E_Z(z)\sin(\omega t + \phi) dz \right| \quad (3)$$

The contribution to the transverse voltage from the vertical magnetic field (B_y(z)) is significantly small. The functions E_x(z) is an even function of z where E_z(z) is an odd function, as shown in Fig. 5.

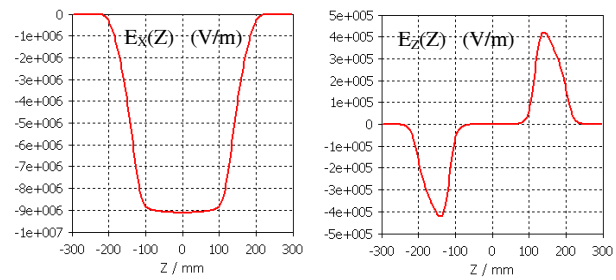

Figure 5: Transverse electric field (left) and longitudinal electric field (right) along the beam line.

The V_T and V_Z seen by a particle with an rf phase of ϕ_s are given by

$$V_T(\phi_s) = V_T^{\max}\sin(\phi_s) \quad (4)$$

$$V_Z(\phi_s) = V_Z^{\max}\cos(\phi_s) \quad (5)$$

The amount of mixing due to any asymmetry, experienced by a particle passing through the beam line depends on the corresponding rf phase of the particle. A crabbing cavity operating at 0 rf phase experiences the highest longitudinal voltage, therefore has maximum effect due to mixing. However for a deflecting cavity operating at $\pi/2$ phase receives minimum effect due to mixing.

OFF-AXIS FIELD ANALYSIS

The deflecting voltage (V_T) is analyzed off-axis (in x and y directions). The normalized deflecting voltage variation shown in Fig. 6, for the 499 MHz design is symmetric in both transverse directions. The change in V_T is given by Eq. 6 for 499 MHz and by Eq. 7 for 400 MHz, where Δx and Δy are the offsets in mm.

$$\frac{V_T}{V_T(r=0)} = \begin{cases} 5.0\times10^{-5}\Delta x^2 + 1.0 \\ -5.0\times10^{-5}\Delta y^2 + 1.0 \end{cases} \quad (6)$$

$$\frac{V_T}{V_T(r=0)} = \begin{cases} 3.0\times10^{-5}\Delta x^2 + 1.0 \\ -3.0\times10^{-5}\Delta y^2 + 1.0 \end{cases} \quad (7)$$

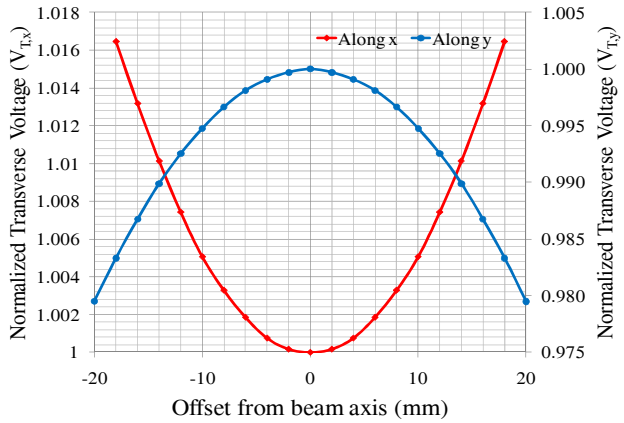

Figure 6: Normalized transverse deflecting voltage variation in x (red) and y (blue) directions.

The small change in V_T clearly shows that the parallel-bar cavity has uniform fields across the beam aperture.

CONCLUSION

A detailed study of numerous design imperfections of the parallel-bar design was performed to determine their effect on mixing between the fundamental deflecting and accelerating modes. The asymmetry in separation between the parallel bars gives a larger longitudinal voltage along the beam axis, yet with a smaller resultant contribution in comparison with the transverse deflecting voltage. Also the analysis of off-axis deflecting voltage shows that the parallel-bar deflecting/crabbing cavity has uniform fields across the beam aperture cross section. The detail analysis shows that the parallel-bar cavity is a robust design in terms of deformations and off-axis field variations.

REFERENCES

[1] J.R. Delayen and H. Wang, Phys. Rev. ST Accel. Beams 12, 062002 (2009).
[2] S.U. De Silva and J.R. Delayen, Proceedings of SRF'09, Berlin, Germany, p. 589 (2009).
[3] S.U. De Silva and J.R. Delayen, Proceedings of IPAC'10, Kyoto, Japan, p. 3075 (2010).
[4] K. Hosoyama *et al*, Proc. of the 7th Workshop on RF Superconductivity, p.547 (1998).